The 6th International Conference on
Engineering Mechanics and Automation (ICEMA 6)
Hanoi, October 15÷16, 2021

Design of UAV system and workflow for weed image segmentation by using deep learning in Precision Agriculture

Duc-Anh Dao, Truong-Son Nguyen, Cong-Hoang Quach, Duc-Thang Nguyen and Minh-Trien Pham*

VNU University of Engineering and Technology, 144 Xuan Thuy, Cau Giay, Hanoi, Vietnam

Abstract— **Collecting and analyzing weed data is crucial, but it is a real challenge to cover a large area of fields or farms while minimizing the loss of plant and weed information. In this regard, Unmanned Aerial Vehicles (UAVs) provide excellent survey capabilities to obtain images of the entire agricultural field with a very high spatial resolution and at a low cost. This paper addresses the practical problem of the weed segmentation task using a multispectral camera mounted on a UAV. We propose the method to find the ideal workflow and system parameters for UAVs to maximize field crop coverage while providing data for reliable and accurate weed segmentation. Around the segmentation task, we examine several Convolutional Neural Networks (CNNs) architectures with different states (fine-tune) to find the most effective one. Besides that, our experiment using Near-infrared (NIR) and Normalized Difference Vegetation Index (NDVI) -the foremost spectroscopies - as an indicator of the vegetation density, health, and greenness. We implemented and evaluated our system on two farms, sugar beet and papaya, to conclude based on each stage of crop growth.**

Keywords*— *UAV, weed segmentation, deep learning, spectroscopy

I. INTRODUCTION

Precision agriculture (PA) can be defined as the science of improving crop yields and assisting management decisions using high technology sensors and analysis tools [1]. PA spatially surveying critical health indicators of crop and applying treatment, e.g., herbicides, pesticides, and fertilizers, only to relevant areas. Because of that, weed treatment is a critical step in PA as it directly associates with crop health and yield. To overcome the above problem, in PA practices, Site-Specific Weed Management (SSWM) is used [2] SSWM focused on dividing the field into management zones where each one receives customized management. Therefore, it is necessary to generate an accurate weed cover map for precise herbicide spraying. Hence, we need to collect high-resolution data image data of the whole field. These images are usually captured by two traditional platforms, satellite, and manned aircraft. However, these conventional platforms present problems related to temporal and spatial resolution, and the successful use of these platforms is dependent on weather conditions [3].

In recent years, along with the development of science and technology, Unmanned Aerial Vehicles (UAVs) are considered a suitable replacement for image acquisition. The use of UAVs to monitor crops offers excellent possibilities to acquire field data in an easy, fast, and cost-effective way compared to previous methods. UAVs can fly at low altitudes and take ultra-high spatial resolution imagery (i.e., a few centimeters), allowing observing small individual plants and patches that are not possible with satellites or piloted aircraft [4]. This significantly improves the performance of the monitoring systems, especially in monitoring and detecting weeds systems. UAVs can serve as an excellent platform to obtain fast and detailed information on arable land when equipped with various sensors. From an orthomosaic map, producers can make beneficial decisions in terms of money and time, monitor the health of plants, get records quickly and accurately on damage or identify potential problems in the field. Moreover, this information is also essential data that enables new technologies such as machine learning, deep learning, etc., to improve productivity in precision agriculture.

Section II presents some common types of UAVs used in the agriculture robotics domain and covers related works using CNN models with multispectral images. Section III describes our proposed method on an available public dataset and details of our deep learning model. Section IV concludes two parts: i) the result of the public dataset, and ii) the procedure for acquiring, calibrating, and evaluating experimental datasets under real conditions. At last, section V concludes the paper.

II. RELATED WORK

In PA, UAVs are inexpensive and easy to use compared to satellites and manned-aircrafts, though limited by insufficient engine power, short flight duration, difficulty in maintaining flight altitude, and aircraft stability [5], [6]. In general, the payload capacity of the UAVs is about 20-30% of its total weight [7], which significantly governs the type of operation

* Corresponding Author: trienpm@vnu.edu.vn (Minh-Trien Pham)

that can be performed with the system. Three major UAVs type can be used for precision weed management: fixed-wing, rotary-wing, and blimps. But the ability to hover in the air and agile manoeuvring makes rotary-wing well-suited to agriculture field inspections. This ability makes rotary-wing UAVs take ultra-high-resolution images and map small individual plants and patches [8]. Although fixed-wing UAVs can fly with high speed [9] and greater payload capacities than the rotary-wing platform, leading to images with coarse-spatial resolution and poor image overlap. Besides fixed-wing and rotary-wing, blimps are also used for obtaining aerial imagery [10]. Blimps are simple UAV platforms where the lift is provided by helium. However, they are not stable under high-speed conditions [11], and the development of highly sophisticated aerial systems (i.e., fixed- and rotary-wing UAVs) are maneuvered easily and attached with in-built sensors/cameras. Because of that, the use of blimps has declined in agricultural applications.

Moreover, one of the most critical parameters in a UAV flight is the altitude above ground level (AGL). It defines the pixel size on the captured images, flight duration and coverage area. It is crucial to determine the spatial quality required for orthomosaics to obtain the ideal pixel size in the images. According to Hengl [12], detecting the smallest object in an image generally requires at least four pixels. When choosing altitude AGL, the spatial resolution must be good enough while covering as many surfaces as possible. Low altitude AGL UAV flights can produce high-resolution images but are limited in the coverage area, thereby increasing flight duration. Therefore, the operation of UAVs is broken down into several flights due to battery life, causing a change in light condition, the unstable appearance of shade, etc.

Several works have been directed using RGB beside multispectral imagery of farming fields to face the substantial similarity in weeds and crops for weed detection technology. [13] using Excess Green Vegetation Index (ExG) [14] and the Otsu's thresholding [15] to remove background (soil, residues). After that, the authors applied a double Hough transform [16] to identify the maincrop lines. To specify crops and weeds, they applied the region-based segmentation method forming a blob coloring analysis. The crop will be any region with at least one pixel belonging to the detected lines; the remaining area means weed. Lambert et al. [17] apply the green normalized differential vegetation index (GNDVI) to classify. The reason for their choice is that high biomass crops such as wheat cause saturation of chlorophyll levels in the red wavelength, resulting in poor performance when using the normalized differential vegetation index (NDVI) [18].

Image segmentation aims to learn information in a given image at a pixel level, an essential but challenging task. In recent years, convolutional neural networks (CNN) have risen as a potent tool for computer vision tasks. The creation of the AlexNet network in 2012 had shown that a large, deep CNN could achieve record-breaking results on a challenging dataset using supervised training [19]. For example, in [20] and [21], authors apply AlexNet for weed detection in different crop fields: soybean, beet, spinach, and bean. Mortensen et al. [22] using a modified version of VGG-16 on the segmentation task of mixed crops from oil radish plots with barley, grass, weed, stump, and soil. However, these methods have a poor performance with low-resolution images because of the sequential max-pooling and down-sampling layers. To solve this issue, U-Net [23] has the mechanic that contracted features will reconstruct the image to input resolution. This paper uses a model based on this U-Net architecture (detailed in Section III-C1).

III. Methods

A. System overview

The main target of the proposed UAV system is to identify plants and weeds in UAV imagery, thereby providing a tool for precisely monitoring real fields. In the following, we will discuss general steps in the preliminary analysis and preparation of the data collection process.

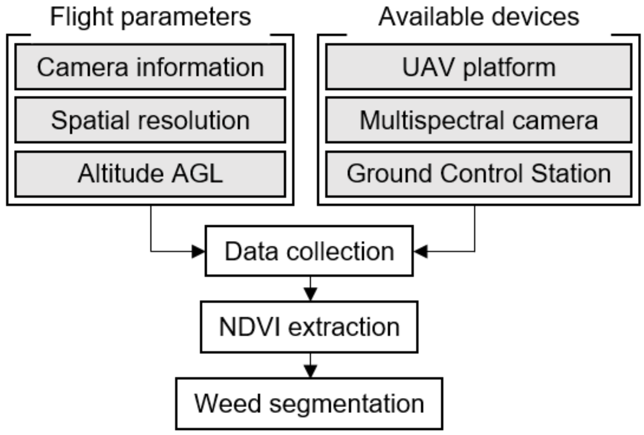

Fig. 1. General overview of the UAVs system used in the image collection process

First of all, it is essential to guarantee safety and accuracy before flying. Devices such as UAVs, computers, and controllers must be checked to see if it is working correctly to avoid system breakdowns and failures due to malfunctions. After that, several parameters need to be calibrated to ensure the UAV is in good condition and ready for take-off. Typically, an inertial measurement unit (IMU), compass, and camera are the things that need calibration. The IMU, including the accelerometer, needs to be calibrated first to establish the standard altitude of the UAV and minimize errors due to inaccurate sensor measurements. Then there is the compass, making sure to avoid potential sources that could affect the magnetometer. For cameras, it is necessary to determine the lens parameters and the types of multispectral cameras before flying. In our case, UAV needs a 2-band multispectral camera (red channel at 660 nm and near-infrared (NIR) at 790 nm) as the minimum required to extract NDVI imagery, a central element in the soil separation task.

In our UAV system, the pilot can serve as Ground Control Point (GCP) to control and send UAV commands from the ground. The UAV sends the real-time images streaming to GCP while in the air; it moves between pre-scheduled waypoints while taking pictures on the ground. Figure 1 illustrates the overview UAVs system using in the image collection process.

B. Dataset and Data Augmentation

This paper uses the crop/weed dataset from a controlled field experiment [24] containing pixel-level annotations of sugar beet and weed images. A multispectral camera Sequoia mounted on a DJI Mavic – commercial MAV, recording datasets at 1 Hz and 2-meter height. A total of 149 images were captured in 3 separate field patches: crop-only, weed-only, and mixed. Each training/test image consisted of the red channel, NIR, and NDVI imagery.

The role of the NDVI spectrum is crucial in the soil segmentation task. The following examples will clarify the importance of NDVI imagery compared to the red channel or NIR in this task. In NIR, we hardly indicate the difference between soil and plant/weed. The red channel image can easily identify the contrast, but it depends on the light conditions when collecting data, causing instability and consistency during training. On the other hand, NDVI imagery is based on how plants reflect certain electromagnetic spectrum ranges, making non-plant materials like soil easily separated. Although the primary contribution of NDVI is used as an indicator of vegetation density, health, and greenness, it has shown excellent results in the ground segmentation task.

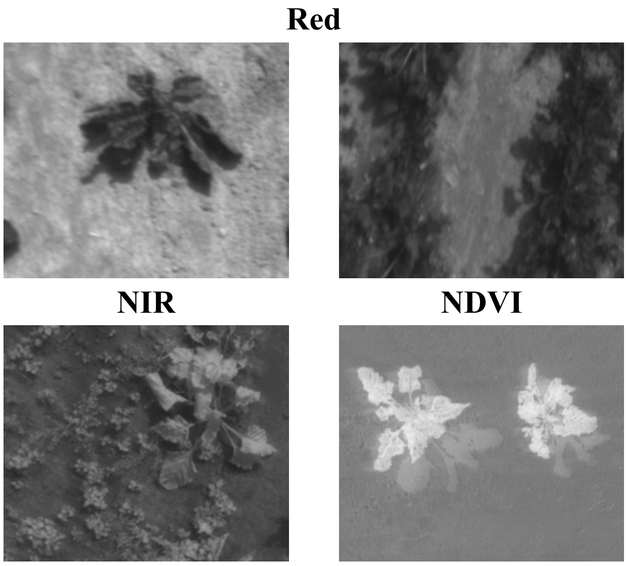

Fig. 2. Red in good light condition (top-left) and bad light condition (top-right). Bottom-left is NIR, and the bottom-right is NDI.

Next, we need to focus on the most crucial task: the distinction between weed and plant. As mentioned before, the training dataset is divided into crop-only and weed-only. The plant has broad leaves, thin twigs, while the weed is small in size and distributed in clusters. It makes the recognition more straightforward in the training process with an individual object. In that case, traditional computer vision or machine learning techniques like the random forest or support vector machine can get the task done. However, while plants often overlap with weeds in practical matters, pixel-by-pixel classification becomes difficult. To address this issue, we decided to use a more advanced solution: a deep learning model due to its robust feature learning and end-to-end training.

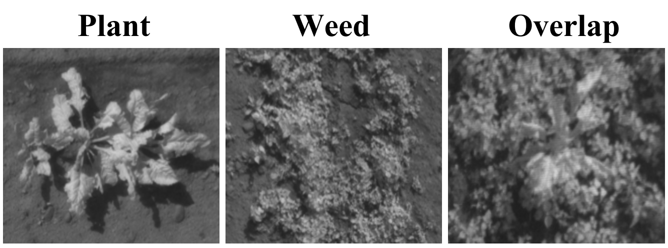

Fig. 3. Individual object: plant (left), weed (middle) and overlapping objects (right).

In our opinion, this dataset has two problems: (i) the quantity is not sufficiently large, and (ii) it impedes the training phase when separating the whole field to crop or weed-only part. To understand these problems, we need to emphasize that deep learning is a powerful tool that can successfully solve many issues related to computer vision. However, one of the significant limitations of this method is the need for large datasets to obtain excellent performance and generalization. Small data can exacerbate specific issues, like overfitting, measurement error, and especially in our case, sampling bias—the weed-only image up to 65% of the entire training set. Therefore, we propose a data augmentation strategy that enriches and removes the bias in this dataset.

TABLE I. NUMBER OF IMAGES AFTER APPLYING DATA AUGMENTATION

Subset	Original dataset	Augmented dataset
Training	125	3564
Testing	24	24
Total	149	3588

The purpose of this strategy is to combine crop-only and weed-only image pairs into one. First, morphological transformations (dilation and erosion) are applied to the crop-only images to remove noise and join separate parts. Then we find external contours, followed by drawing a rectangle mask for each of them. Finally, we use the alpha blending technique (alpha=1) to overlay the crop over the weed image. Figure 4 illustrates the augmentation strategy, and each class is labeled as follows {background, crop, weed} = {black, green, red}. The number of images generated after using data augmentation is shown in Table I.

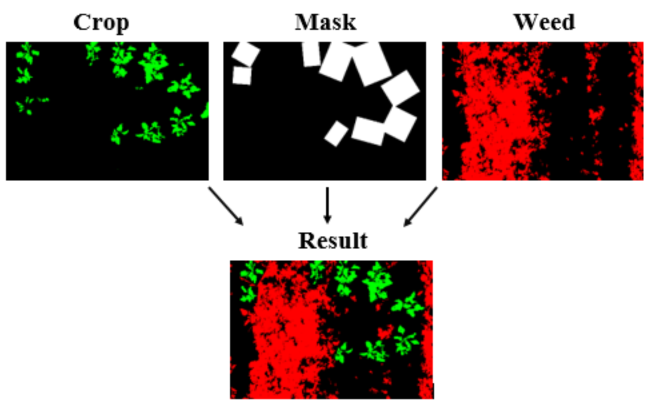

Fig. 4. Example of data augmentation.

C. *Modified U-Net Architecture with residual unit*

1) *U-Net*

U-Net is a deep learning model proposed for the image segmentation task. Its architecture creates a route for information propagation, thus using low-level details while retaining high-level information. It has the contraction (encoder) and expansion (decoder) paths, creating the unique U-shape. Each encoder layer comprises two convolution layers with Rectified Linear Units (ReLU) activation functions followed by max-pooling operation. Stacks of those layers will learn features of increasing complexity levels while simultaneously performing downsampling. On the other hand, the decoder up-sample also appends feature maps of the corresponding encoder to combine global information with precise localization. The network's output has the same width and height as the original image, with a depth indicating each label's activation. For our segmentation mission, there are three classes: crop, weed, and soil.

2) Hybrid with the residual unit

Training neural networks with many deep layers would improve the model performance. However, that depth usually causes the vanishing gradient problem and makes it unable to propagate useful gradient information throughout the model. To address the degradation problem, He et al. [25] introduced a deep residual learning framework. Instead of letting layers learn the underlying mapping H(x) where x is the input of the first layer, the network will fit F(x) = H(x)-x which gives H(x) = F(x) + x. Although both methods could approximate the desired functions, the ease of training with residual functions is much better. With all that said, the model we use in this paper combines the strengths of both U-Net and the residual unit (ResBlock), and we call it the ResUNet model.

IV. EXPERIMENTAL RESULTS

A. Dataset Result

For quantitative evaluation, we use the F1 score (3) as the harmonic mean of the recall and precision, which gives an overall result on the network's positive labels.

$$F1 = 2.\frac{Precision\,.Recall}{Precision + Recall} \tag{3}$$

Where *precision* measures how accurate the neural network was at positive observations, and *recall* measures how effectively the neural network identified the target.

TABLE II. Performance comparison of 6 models

Resolution	F1 Score (%)					
	CNN	DeepLabV3	HSCNN	UNet	SegNet	ResUNet
256 x 256	64.29	58.01	66.36	66.16	69.11	**73.87**
512 x 512	66.76	68.91	77.15	77.78	75.23	**80.56**

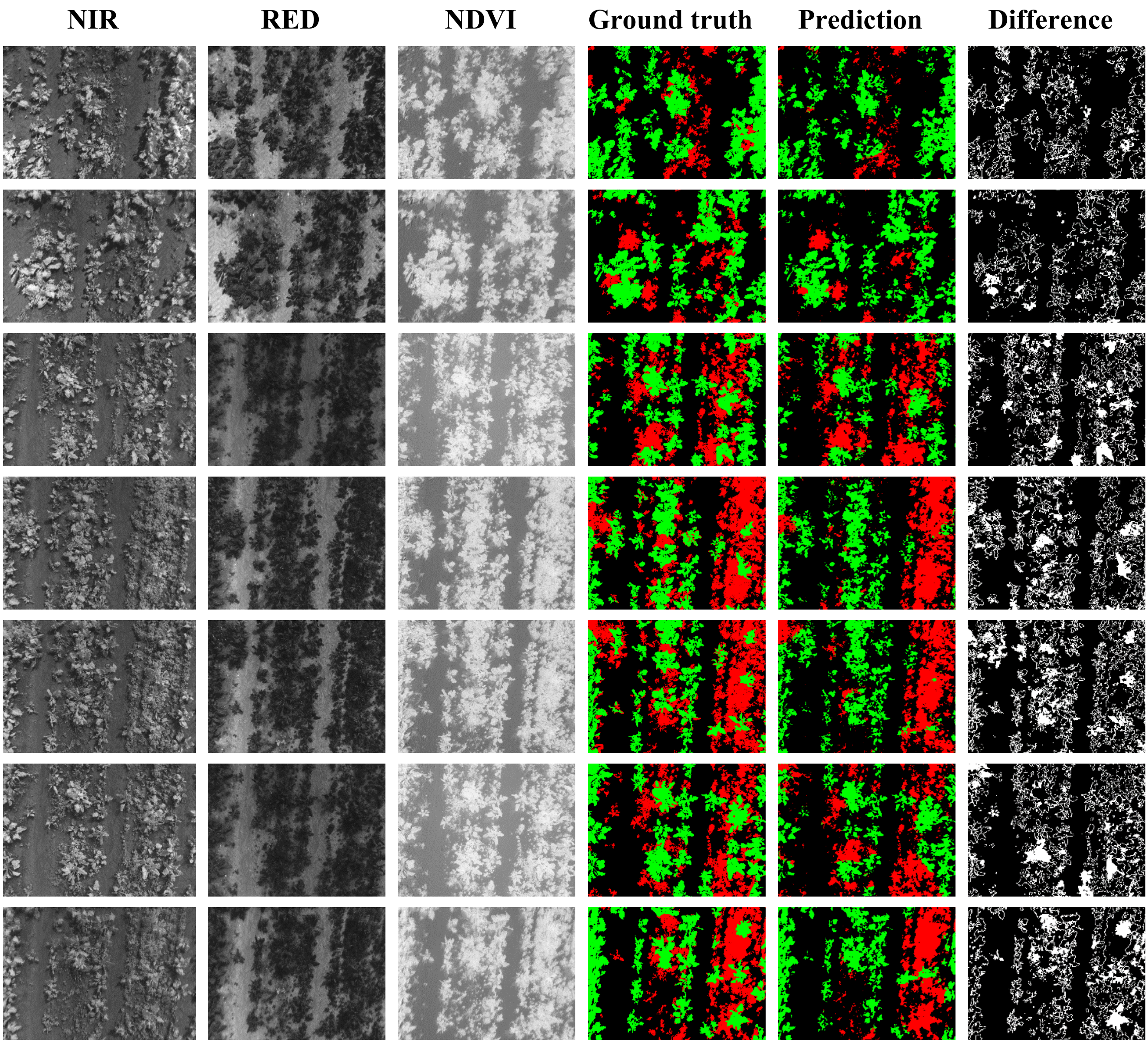

Fig. 5. Result of some examples (row-wise). The first three columns are the input of the model. The fourth and fifth columns are showing ground truth and the prediction. The last column is the difference between ground truth and prediction mask.

* Corresponding Author: trienpm@vnu.edu.vn (Minh-Trien Pham)

Table II shows the results of the proposed method. We chose to experiment with multiple resolutions because we wanted to simulate the altitude of the UAV when collecting data: lower resolutions taken at high altitudes would cover a wider field, thereby reducing sampling time. However, in return, it will lose detailed features of crops and weeds, directly affecting the final result of models.

In Sections II and III-C, we have presented the strengths and limitations of the models. The experimental results in Table II have demonstrated that CNNs are not suitable for complex tasks like segmentation. In contrast, ResUNet has shown its superiority when increasing accuracy by 3-4% compared to the second-best model. However, the numbers cannot summarize the entire results. We need to have specific illustrations to analyze this result more closely.

For visual examination, we present some examples of input data and the difference between ground truth and model probability (Fig. 5). The 3-channel input image is represented by the first three columns of spectral types: NIR, RED, and NDVI. The following two columns are the ground-truth annotation image and our probability output; each class is labeled as follows {background, crop, weed} = {black, green, red}. Finally, the last column gives a detailed look at the mistakes we encountered. The difference between ground truth and prediction images is shown in white pixels; the fewer white pixels an image has, the more accurate it is. It can be seen that misclassification areas of weed and crop appear with a low number. That case mainly occurs when dense areas of these two types overlap. This shows that our model needs improvement in some parameters, but overall the classification results are satisfactory. Besides that, there is significant misclassification in boundary areas occurring in both crops and weeds. In our opinion, the proposed spatial resolution and sampling frequency in the data acquisition process are not suitable. The poor spatial resolution makes the data not detailed enough to feed the segmentation model. High sampling frequency causes motion-blur phenomenon, which appears many times in this dataset. These factors induce the degradation of image quality, causing poor performance of the predictive model.

Besides illustrable errors, we are still investigating other factors that affect classification performance. We suspect it is due to i) shadow noises appearing in most of the input images, ii) the absence of green and blue channels in the dataset. Shadows can reduce or lose all information in remote sensor images. That missing information content can render remote estimation of biophysical parameters inaccurate and prevents image interpretation [26]. Besides that, some papers using just RGB images from UAV [27], [28] can get great results, which led us to consider the underappreciated role of green and blue images in this dataset. However, since the scope of this paper can hardly reach such content, we would like this issue to future work and will be studied carefully.

B. Experiment

After verifying the model with the available datasets, we conducted experiments to verify the model under real conditions. In this experiment, the UAV was installed with a camera capable of capturing spectral images and flying at different altitudes. This data will then be calibrated before being fed into the deep learning model. And finally, the results of the model and analyze the results to make judgments about system parameters with data and model.

1) System Setting

To collect the data, we used a MapIR Survey3W multispectral camera mounted on the DJI Mavic 2 Enterprise, as shown below.

(a) (b)

Fig. 6. System components: (a) Mavic 2 Enterprise and MapIR Survey3W. (b) MapIR Survey3W

MapIR Survey3W is a low-cost multispectral camera. Its 12MP sensor and sharp non-fisheye lens (with -1% extreme low distortion glass lens allow it to capture aerial media efficiently. It has an 87° HFOV (19mm) f/2.8 aperture. In this experiment, we collect data for 3 wavelength bands, Near-Infrared 850nm, Red 660nm, and Green 550nm, at different heights of 3 meters, 5 meters, and 8 meters.

2) Data calibration

As we all know, our sun emits a large spectrum of light reflected by objects on the Earth's surface. A camera can be used to capture this reflected light in the wavelengths that the camera's sensor is sensitive to. We supply sensors based on silicon sensitivity in the Visible and Near-Infrared spectrum from about 400-1200nm. Using band-pass filters that only allow a narrow range of light to reach the sensor, we can capture the amount of reflectance of objects to that band of light. So, therefore, the image we obtain is always dependent on the ambient light conditions. In each different flight, the resulting image will have various reflection qualities and to solve that problem, we use a calibration board as shown below.

Fig. 7. Calibrated Reflectance Panel (CRP)

To determine the transfer function, first convert the raw pixels of the panel image to units of radiance. Then calculate the average value of radiance for the pixels located inside the panel area of the image. The transfer function of radiance to reflectance for the i-th band is:

$$F_i = \frac{\rho_i}{avg(L_i)} \tag{4}$$

Where F_i is the reflectance calibration factor for band i, ρ_i is the average reflectance of the CRP for the i-th band (from the calibration data of the panel provided) is the average value of the radiance for the pixels inside the panel for band i. After performing the correction, we will proceed to calculate the NDVI by:

$$NDVI = \frac{NIR - RED}{NIR + RED} \quad (5)$$

Here are a few experimental images:

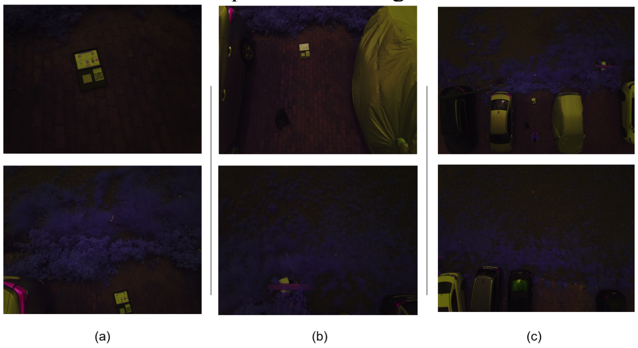

Fig. 8. Images of CRP and data samples at different heights: (a) 3 meter, (b) 5 meter and (c) 8 meter

Here are data after calibration:

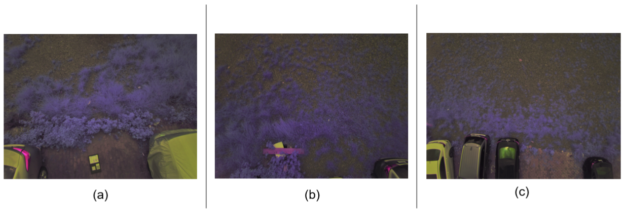

Fig. 9. Data after calibration at different heights: (a) 3 meter, (b) 5 meter and (c) 8 meter

3) Result

Experiments were conducted on papaya fields. There are a small number of immature papaya plants along with two kinds of weeds: *common chickweed* (Stellaria media) and *crabgrass* (Digitaria) (Fig. 10). We took 110 images at three different altitudes with a resolution of 4000 x 3000 pixels. The supervised dataset was annotated manually by science experts. This process took up about 45 minutes/image on average. After training the ResUNet model, we obtain an F1-score: 0.82, 0.64, 0.61 at altitudes of 3, 5, and 8 meters, respectively.

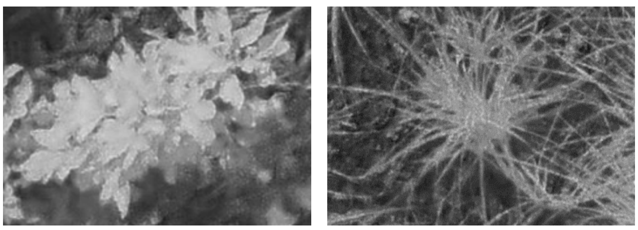

Fig. 10. Chickweed (left) and crabgrass (right)

The weed that appears much in this data set is chickweed. The morphological features of this weed are very similar to immature papaya. The difference is the size of weed leaves is smaller, and they grow denser than papaya. We find this is a challenging dataset with such slight differences and can only be completed when the image is sufficiently detailed. Our experiments show that only images taken at 3 meters (among the three experimental heights, 3, 5, and 8 meters) can detect plants (Fig. 11). It is entirely reasonable because a ground resolution of 0.2 mm/px (3 meters height and a resolution of 4000 x 3000 pixels) makes the images highly detailed and eligible to distinguish immature papaya plants from chickweed.

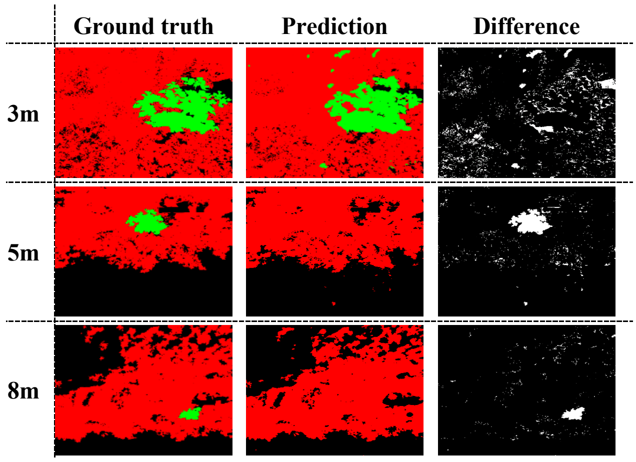

Fig. 11. The difference between ground truth and the model's prediction at different heights: 3, 5, and 8 meters (row-wise).

Though, that does not mean all data at an altitude of 5 or 8 meters is ineffective in practice. As we mentioned earlier, this dataset was challenging, and the crops were out of season at the time of data collection. That leads to many areas of dense weeds and overlapping between those areas and plants. Therefore, the images at 5 or 8 meters are not eligible for the segmentation task in this particular circumstance. However, in many practical cases, plant and weed classification is often implemented early to prevent the spread of weeds (early site-specific weed management (ESSWM)). In those cases, early-stage weeds sparsely grow, and overlapping objects appear with lower frequency. That makes the segmentation task more straightforward and suitable for high-altitude images as they can cover large fields, improving classification productivity while maintaining accuracy.

V. Conclusions

UAVs used in weed segmentation applications must distinguish crops from weeds to make interventions at the right time. This paper uses multispectral imagery to focus on papaya (our dataset) and sugar beet crops (public dataset). We trained six different models and evaluated them by using F1-score as a metric. Then, an assessment was performed by visually comparing ground truth with probability outputs. The proposed approach achieved an acceptable performance of 0.82 and 0.81 F1-score for papaya and sugar beet fields, respectively.

Our experiment has solved the practical problem of using UAV images for weed segmentation by deep learning. We have proposed a good workflow, and the UAV parameters were calculated and adjusted thoughtfully. From that, we produced acceptable results even on difficult classification conditions. Our UAV system at three different heights achieves remarkable results in weed detection and can fix the misclassification in boundary areas (section IV-A). More specifically, when plants and weeds have similar morphological/color features and high weeds density, the dataset should be captured at 3 meters height to preserve the details. In cases like ESSWM, 5 or 8 meters may be appropriate to optimize crop area management while ensuring classification quality.

We will further study the factors affecting the final classification results and make a clearer statement about the high-altitude UAV systems in different crop growth stages. To address this, we required more training data on large-scale, multiple weed varieties over longer periods of time to develop a weed detector with more efficient strategies. We are planning to build an extensive dataset to support future work in the agriculture robotics domain.

ACKNOWLEDGMENT

Quach Cong Hoang was funded by Vingroup Joint Stock Company and supported by the Domestic Ph.D. Scholarship Programme of Vingroup Innovation Foundation (VINIF), Vingroup Big Data Institute (VINBIGDATA), code VinIF 2020. TS.23.

REFERENCES

[1] P. Singh *et al.*, “Hyperspectral remote sensing in precision agriculture: present status, challenges, and future trends,” in *Hyperspectral Remote Sensing*, Elsevier, 2020, pp. 121–146.

[2] D. C. Tsouros, S. Bibi, and P. G. Sarigiannidis, “A review on UAV-based applications for precision agriculture,” *Inf.*, vol. 10, no. 11, 2019.

[3] F.-J. Mesas-Carrascosa *et al.*, “Assessing Optimal Flight Parameters for Generating Accurate Multispectral Orthomosaicks by UAV to Support Site-Specific Crop Management,” *Remote Sens. 2015, Vol. 7, Pages 12793-12814*, vol. 7, no. 10, pp. 12793–12814, Sep. 2015.

[4] J. Torres-Sánchez, J. M. Peña-Barragán, D. Gómez-Candón, A. I. De Castro, and F. López-Granados, “Imagery from unmanned aerial vehicles for early site specific weed management,” *Wageningen Acad. Publ.*, pp. 193–199, 2013.

[5] P. J. Hardin and T. J. Hardin, “Small-scale remotely piloted vehicles in environmental research,” *Geogr. Compass*, vol. 4, no. 9, pp. 1297–1311, 2010.

[6] A. S. Laliberte, A. Rango, and J. Herrick, “Unmanned aerial vehicles for rangeland mapping and monitoring: A comparison of two systems,” *Am. Soc. Photogramm. Remote Sens. - ASPRS Annu. Conf. 2007 Identifying Geospatial Solut.*, vol. 1, pp. 379–388, 2007.

[7] S. Nebiker, A. Annen, M. Scherrer, and D. Oesch, “A light-weight multispectral sensor for micro UAV—Opportunities for very high resolution airborne remote sensing,” *Int. Arch. Photogramm. Remote Sens. Spat. Inf. Sci.*, vol. 37, no. Vi, pp. 1193–1200, 2008.

[8] H. Xiang and L. Tian, “Development of a low-cost agricultural remote sensing system based on an autonomous unmanned aerial vehicle (UAV),” *Biosyst. Eng.*, vol. 108, no. 2, pp. 174–190, Feb. 2011, doi: 10.1016/J.BIOSYSTEMSENG.2010.11.010.

[9] A. Frank, J. S. McGrew, M. Valenti, D. Levine, and J. P. How, “Hover, transition, and level flight control design for a single-propeller indoor airplane,” *AIAA Guid. Navig. Control Conf.*, vol. 1, pp. 100–117, 2007, doi: 10.2514/6.2007-6318.

[10] D. Vericat, J. Brasington, J. Wheaton, and M. Cowie, “Accuracy assessment of aerial photographs acquired using lighter-than-air blimps: LOW-cost tools for mapping river corridors,” *River Res. Appl.*, vol. 25, no. 8, pp. 985–1000, Oct. 2009, doi: 10.1002/RRA.1198.

[11] J. Everaerts, “The use of unmanned aerial vehicles (UAVs) for remote sensing and mapping,” *Int. Arch. Photogramm. Remote Sens. Spat. Inf. Sci.*, vol. 37, no. March, pp. 1187–1192, 2008.

[12] T. Hengl, “Finding the right pixel size,” *Comput. Geosci.*, vol. 32, no. 9, pp. 1283–1298, 2006.

[13] C. Gée, J. Bossu, G. Jones, and F. Truchetet, “Crop/weed discrimination in perspective agronomic images,” *Comput. Electron. Agric.*, vol. 60, no. 1, pp. 49–59, Jan. 2008.

[14] D. M. Woebbecke, G. E. Meyer, K. Von Bargen, and D. A. Mortensen, “Color indices for weed identification under various soil, residue, and lighting conditions,” *Trans. Am. Soc. Agric. Eng.*, vol. 38, no. 1, pp. 259–269, 1995.

[15] N. Otsu *et al.*, “A Threshold Selection Method from Gray-Level Histograms,” *IEEE Trans. Syst. Man. Cybern.*, vol. C, no. 1, pp. 62–66, 1979.

[16] P.V.C. Hough, “Method and means for recognizing complex patterns,” *U.S. Patent 30696541962*. Dec. 18, 1962.

[17] J. P. Lambert, D. Z. Childs, and R. P. Freckleton, “Testing the ability of unmanned aerial systems and machine learning to map weeds at subfield scales: a test with the weed Alopecurus myosuroides (Huds),” *Pest Manag. Sci.*, vol. 75, no. 8, pp. 2283–2294, Aug. 2019.

[18] A. A. Gitelson, Y. J. Kaufman, and M. N. Merzlyak, “Use of a green channel in remote sensing of global vegetation from EOS-MODIS,” *Remote Sens. Environ.*, vol. 58, no. 3, pp. 289–298, Dec. 1996.

[19] KrizhevskyAlex, SutskeverIlya, and H. E., “ImageNet classification with deep convolutional neural networks,” *Commun. ACM*, vol. 60, no. 6, pp. 84–90, May 2017.

[20] A. dos Santos Ferreira, D. Matte Freitas, G. Gonçalves da Silva, H. Pistori, and M. Theophilo Folhes, “Weed detection in soybean crops using ConvNets,” *Comput. Electron. Agric.*, vol. 143, no. February, pp. 314–324, 2017.

[21] M. D. Bah, E. Dericquebourg, A. Hafiane, and R. Canals, *Deep learning based classification system for identifying weeds using high-resolution UAV imagery*, vol. 857. Springer International Publishing, 2019.

[22] A. K. Mortensen, M. Dyrmann, H. Karstoft, R. N. Jørgensen, and R. Gislum, “Semantic segmentation of mixed crops using deep convolutional neural network.,” *CIGR-AgEng Conf. 26-29 June 2016, Aarhus, Denmark. Abstr. Full Pap.*, pp. 1–6, 2016.

[23] O. Ronneberger, P. Fischer, and T. Brox, “U-Net: Convolutional Networks for Biomedical Image Segmentation,” *Med. Image Comput. Comput. Interv.*, vol. 9351, pp. 234–241, May 2015.

[24] I. Sa *et al.*, “WeedNet: Dense Semantic Weed Classification Using Multispectral Images and MAV for Smart Farming,” *IEEE Robot. Autom. Lett.*, vol. 3, no. 1, pp. 588–595, Jan. 2018.

[25] K. He, X. Zhang, S. Ren, and J. Sun, “Deep Residual Learning for Image Recognition,” *Proc. IEEE Comput. Soc. Conf. Comput. Vis. Pattern Recognit.*, vol. 2016-Decem, pp. 770–778, Dec. 2015.

[26] P. M. Dare, “Shadow analysis in high-resolution satellite imagery of urban areas,” *Photogramm. Eng. Remote Sensing*, vol. 71, no. 2, pp. 169–177, 2005.

[27] H. Huang *et al.*, “Accurate Weed Mapping and Prescription Map Generation Based on Fully Convolutional Networks Using UAV Imagery,” *Sensors*, vol. 18, no. 10, p. 3299, Oct. 2018, doi: 10.3390/S18103299.

[28] M. D. Bah, A. Hafiane, and R. Canals, “Deep Learning with Unsupervised Data Labeling for Weed Detection in Line Crops in UAV Images,” *Remote Sens.*, vol. 10, no. 11, p. 1690, Oct. 2018, doi: 10.3390/RS10111690.